frontiers in Endocrinology

ORIGINAL RESEARCH
published: 04 February 2020
doi: 10.3389/fendo.2020.00029

Stathmin-2 Mediates Glucagon Secretion From Pancreatic α-Cells

Farzad Asadi[1] *and Savita Dhanvantari*[1,2,3]*

[1] Department of Pathology and Laboratory Medicine, Schulich School of Medicine & Dentistry, Western University, London, ON, Canada, [2] Department of Medical Biophysics, Western University, London, ON, Canada, [3] Lawson Health Research Institute, London, ON, Canada

Inhibition of glucagon hypersecretion from pancreatic α-cells is an appealing strategy for the treatment of diabetes. Our hypothesis is that proteins that associate with glucagon within alpha cell secretory granules will regulate glucagon secretion, and may provide druggable targets for controlling abnormal glucagon secretion in diabetes. Recently, we identified a dynamic glucagon interactome within the secretory granules of the α cell line, αTC1-6, and showed that select proteins within the interactome could modulate glucagon secretion. In the present study, we show that one of these interactome proteins, the neuronal protein stathmin-2, is expressed in αTC1-6 cells and in mouse pancreatic alpha cells, and is a novel regulator of glucagon secretion. The secretion of both glucagon and Stmn2 was significantly enhanced in response to 55 mM K^+, and immunofluorescence confocal microscopy showed co-localization of stathmin-2 with glucagon and the secretory granule markers chromogranin A and VAMP-2 in αTC1-6 cells. In mouse pancreatic islets, Stathmin-2 co-localized with glucagon, but not with insulin, and co-localized with secretory pathway markers. To show a function for stathmin-2 in regulating glucagon secretion, we showed that siRNA—mediated depletion of stathmin-2 in αTC1-6 cells caused glucagon secretion to become constitutive without any effect on proglucagon mRNA levels, while overexpression of stathmin-2 completely abolished both basal and K^+-stimulated glucagon secretion. Overexpression of stathmin-2 increased the localization of glucagon into the endosomal-lysosomal compartment, while depletion of stathmin-2 reduced the endosomal localization of glucagon. Therefore, we describe stathmin-2 as having a novel role as an alpha cell secretory granule protein that modulates glucagon secretion via trafficking through the endosomal-lysosomal system. These findings describe a potential new pathway for the regulation of glucagon secretion, and may have implications for controlling glucagon hypersecretion in diabetes.

Keywords: glucagon, alpha cell, glucagon hypersecretion, glucagon interactome, stathmin-2

OPEN ACCESS

Edited by:
Magalie A. Ravier, INSERM U1191 Institut de Génomique Fonctionnelle (IGF), France

Reviewed by:
Andrei I. Tarasov, University of Oxford, United Kingdom
Albert Salehi, Lund University, Sweden

***Correspondence:**
Savita Dhanvantari
sdhanvan@lawsonimaging.ca

Specialty section:
This article was submitted to Diabetes: Molecular Mechanisms, a section of the journal Frontiers in Endocrinology

Received: *06 November 2019*
Accepted: *14 January 2020*
Published: *04 February 2020*

Citation:
Asadi F and Dhanvantari S (2020) Stathmin-2 Mediates Glucagon Secretion From Pancreatic α-Cells. Front. Endocrinol. 11:29. doi: 10.3389/fendo.2020.00029

INTRODUCTION

Hyperglucagonemia is a characteristic sign of diabetes, causing fasting hyperglycemia and glycemic volatility. Clinically, glycemic variability contributes to the development of diabetes complications (1). Persistent hyperglucagonemia may exacerbate abnormal glucose metabolism in patients with type 2 diabetes and lead to metabolic disturbances in obese and prediabetic individuals (2). Further

complicating glucose homeostasis in diabetes is the direct effect of glucose on the alpha cells; while glucagon secretion is maximally suppressed at plasma glucose concentrations of 5–10 mM, it increases at glucose levels above 10 mM, thus exacerbating hyperglycemia (3–6). Therefore, controlling excess glucagon secretion may be a potential therapeutic strategy for diabetes (7) so that glycemia and glucose metabolism may be better regulated. Such an approach has been suggested as a priority for the treatment of diabetes (1).

Combating hyperglucagonemia could be theoretically achieved by (i) inhibition of glucagon action at target organs by blocking the glucagon receptor, or (ii) inhibition of glucagon secretion from the pancreatic α cells. While in the short-term the former could be an effective therapeutic strategy, it can lead to α cell hyperplasia and hyperglucagonemia over a long-term period (8), along with a risk of hypoglycemia (9) and disturbances in lipid metabolism (10). Therefore, inhibiting glucagon secretion, rather than blocking the glucagon receptor, may be a more appropriate therapeutic approach for the treatment of hyperglucagonemia of diabetes (11).

It has been documented that suppression of glucagon secretion can be mediated at the systemic, paracrine or intrinsic level (12). As a systemic modulator, GLP-1 inhibits glucagon secretion; however, there are controversies as to whether GLP-1 directly inhibits glucagon secretion from α cells by signaling through the alpha cell GLP-1R (13–15), or indirectly by increasing inter-islet somatostatin or insulin secretion (13, 16). Glucagon secretion is also suppressed by paracrine signaling through the insulin, somatostatin and $GABA_A$ receptors on the α cell (16–18) At an intrinsic level, glucose directly or indirectly inhibits glucagon secretion from the α cell (19–22) by altering downstream activities of Ca^{2+} channels, K_{ATP} channels (23), and trafficking of secretory granules (24).

We are pursuing the hypothesis that glucagon secretion can also be controlled by proteins within the secretory granule that associate with glucagon. By conducting secretory granule proteomics in αTC1-6 cells, we have recently described a dynamic glucagon interactome, and shown that components of this interactome can play a role in modulating glucagon secretion (25). Of these components, a protein of particular interest is Stathmin-2 (Stmn2 or SCG10), a member of the stathmin family of Golgi proteins (26) that may play a role in the regulation of neuroendocrine secretion (27). In the human islet, Stmn2 expression may be unique to alpha cells, as shown by genome-wide RNA-Seq analysis (28) and single cell transcriptomics (23), and alpha cell Stmn2 mRNA expression is differentially regulated in type 2 diabetes (29). These studies, together with our proteomics findings, led us to hypothesize that Stmn2 may function in α cells to modulate glucagon secretion. In the present study, we show that Stmn2 is co-localized with glucagon in secretory granules of αTC1-6 cells and controls glucagon secretion by trafficking through the endosomal/lysosomal system.

MATERIALS AND METHODS

Cell Culture

αTC1-6 cells (a kind gift from C. Bruce Verchere, University of British Columbia, Vancouver, BC, Canada) were cultured in regular DMEM medium containing 5.6 mM glucose (Cat# 12320032, Thermo Fisher Scientific) supplemented with 15% horse serum (Cat# 26050088, Thermo Fisher Scientific), 2.5% FBS (Cat# 16000044, Thermo Fisher Scientific), L-glutamine and sodium pyruvate. For secretion experiments, cells were plated in 6 –well plates and for all experiments, a low passage number (up to P6) was used. Twenty-four hours prior to secretion experiments, media were removed and replaced with DMEM without supplements. To evaluate (25) the regulated secretion of glucagon, cells were washed twice with HBSS, pre-incubated for 2 h in DMEM without supplements, then incubated for 15 min with or without KCl (55 mM). These media were collected into tubes containing protease inhibitor (PMSF, 45 mM) and phosphatase inhibitors (sodium orthovanadate, 1 mM; and sodium fluoride 5 mM) while tubes were kept on ice. After collection, media were centrifuged at 13,000×g for 5 min at 4°C, and the supernatant was collected into new microfuge tubes and immediately kept at −80°C until analysis. After media were removed, cells were washed using ice-cold PBS (pH 7.4) and lysed in RIPA buffer (Cat# 89900, Thermo Fisher Scientific) containing abovementioned protease and phosphatase inhibitors. The lysed cells were centrifuged at 13,000×g for 5 min at 4°C and the supernatant was kept at −80°C for protein assays.

Gene Construct and Plasmid Preparation

To generate the expression plasmid for Stmn2, the Kozak sequence (GCCACC), signal peptide sequence and coding sequence of mouse Stmn2 (https://www.uniprot.org/uniprot/P55821) were ligated into the NheI and ApaI restriction sites of pcDNA3.1(+) MAr. The construct was synthesized by GENEART GmbH, Life Technologies (GeneArt project 2018AAEGRC, Thermo Fisher Scientific). Then, Max Efficiency DH5α competent cells (Thermo Fisher Scientific, Cat# 18258012) were transformed according to the manufacturer's protocol. Plasmids were then extracted and purified using the PureLink HiPure Plasmid Maxiprep Kit (Thermo Fisher Scientific, Cat# K210006) for downstream experiments. Correct assembly of the final construct was verified by gene sequencing at the London Regional Genomics Facility, Western University. For Stmn2 overexpression studies, αTC1-6 cells were transiently transfected by pcDNA3.1 (+) MAr-stmn2 construct or empty vector (negative control). All transfections were done using Lipofectamine 2000 (Cat#11668-027, Invitrogen). To monitor normal cell growth and morphology, cells were checked daily by the EVOS cell imaging system (Thermo Fisher Scientific). The efficiency of transfection was determined at >70% through co-transfection with pEGFP.

Gene Silencing Experiments

siRNA-Mediated Depletion of Stathmin-2

Functional analysis of Stmn2 was done by gene silencing experiments. siRNAs targeting three regions within the Stmn2

mRNA (Cat# s73356, s73354, s73355) were chosen from pre-designed mouse siRNAs (Silencer siRNA, Thermo Fisher Scientific). The control group was treated with Mission siRNA Universal Negative Control # 1 (Cat# SIC001, Sigma-Aldrich). Gene silencing was done based on a previously published protocol (30) and as we have done previously with some modifications (25). Briefly, αTC1-6 cells were cultured in regular DMEM to 60% confluency. Media were removed and replaced with 2 mL Opti-MEM (Cat# 31985-070, Gibco) containing 50 nM pooled siRNAs with Lipofectamine 2000. After 8 h, media were changed to regular DMEM without FBS and cultured for 72 h. Then, media were refreshed and cells were cultured for 15 min in the absence or presence of 55 mM KCl as described above. Gene silencing was confirmed by analyzing mRNA expression levels of Stmn2. After removing media, cells were washed by cold PBS (pH 7.4) and total RNA was extracted (RNeasy extraction kit; Cat # 74104, Qiagen). cDNA synthesis was performed using the SuperScript III First Strand Synthesis Supermix for qRT-PCR (Cat # 11752050, Thermo Fisher Scientific), according to the supplier's protocol. Real-time PCR was performed using Quant Studio Design and Analysis Real-Time PCR Detection System in conjunction with the Maxima SYBR Green qPCR Master Mix (Cat # K0221, Thermo Fisher Scientific) using specific primers for Stmn2: forward, 5′-GCAATGGCCTACAAGGAAAA-3′; reverse, 5′-GGTGGCTTCAAGATCAGCTC-3′; and β-Actin; forward, 5′-AGCCATGTACGTAGCCATCC-3′; reverse, 5′-CTCTCAGC TGTGGTGGTGAA-3′. Gene expression levels for stathmin-2 were normalized to that of β-Actin. The normalized level of transcripts in the depleted cells was shown relative to that of the non-targeting negative control. Relative expression levels were determined as percent of alterations compared to the control. Statistical analysis was performed using *t*-test at $\alpha = 0.05$.

Proglucagon Gene Expression Levels Following Stmn2 Depletion

After siRNA treatments, proglucagon gene expression levels were measured by real-time PCR as described above using proglucagon-specific primers (forward: 5′-CAGAGGAG AACCCCAGATCA-3′, reverse: 5′-TGACGTTTGGCAATGT TGTT-3′).

Immunoblotting

To test for effects of siRNA transfection on levels of Stmn2, α-TC1-6 cells were lysed using non-ionic lysis buffer (50 mM Tris pH 7.4, 150mM NaCl, 1% Triton X-100 plus cOmplete Mini Protease Inhibitor Cocktail and 5 μg/mL Aprotinin). Proteins were resolved by 4-12% NuPAGE gel (Cat # NP0335Box, Invitrogen), transferred to a PVDF membrane (Cat # IB401001, Invitrogen) and probed with primary antibodies (Stmn2, Cat# 720178, Thermo Fisher Scientific; 1:1000; beta actin, Cat# ab8227, Abcam, 1:1000) overnight. Immunoreactive bands were visualized using HRP-conjugated goat anti-rabbit secondary antibody (Cat# 31460, Invitrogen; 1:1000) and Clarity Western ECL substrate (Cat# 170-5061, Bio-Rad). Images were acquired on a BioRad ChemiDoc Imaging System. Total cell extracts from control cells were used as positive control.

Immunofluorescence Confocal Microscopy

αTC1-6 Cells

To determine if Stmn2 and glucagon could be co-localized to the same intracellular compartments, we used immunofluorescence confocal microscopy. Wild type αTC1-6 cells were seeded on collagen (type I)-coated coverslips and grown in regular DMEM, then incubated in non-supplemented DMEM for 24 h. At the end of incubation, cells were washed once with PBS, fixed in 2% paraformaldehyde (in PBS) for 30 min, permeabilized with 0.25% Triton X-100 (in PBS) for 5 min and washed with PBS. After 1 h incubation with blocking buffer (10% goat serum in 1% BSA/PBS), coverslips were incubated with primary antibodies against glucagon (mouse anti- glucagon antibody, Cat # ab10988, Abcam; 1:1000), Stathmin-2 (goat anti-SCG10 antibody, Cat # ab115513, Abcam; 1:1000), secretory granule marker, chromogranin A (mouse anti-ChgA antibody, Cat# MAB319, Sigma; 1:1000), secretory granule marker, VAMP2 (rabbit anti-VAMP2, Cat# ab215721, Abcam; 1:1000), early endosome marker, EEA1 (rabbit antiEEA1, Cat # ab 2900, Abcam; 1:500) or the lysosomal marker, Lamp2A (rabbit anti-Lamp2A, Cat# ab18528, Abcam; 1:500) overnight. After washing with PBS, coverslips were incubated with the following secondary antibodies as appropriate: goat anti-mouse IgG Alexa Fluor 488 (Cat# A-11001, Molecular Probes; 1:500), goat anti-rabbit IgG Alexa Fluor 594 (Cat# A11037, Invitrogen; 1:500) or donkey anti-goat IgG Alexa Fluor 555 (Cat# ab150130, Abcam; 1:500) Invitrogen) for 2 h in the dark at room temperature. Then, coverslips were washed with PBS and mounted on glass slides using DAPI containing ProLong antifade mountant (Cat # P36935, Molecular Probes) for image analysis by confocal immunofluorescence microscopy (Nikon A1R, Mississauga, Canada). Coverslip preparation was done at four different times with freshly thawed cells.

Mouse Pancreatic Islets

All mice were treated in accordance with the guidelines set out by the Animal Use Subcommittee of the Canadian Council on Animal Care at Western University based on the approved Animal Use Protocol AUP 2012-020. Six to eight-week old male C57BL/6 mice ($n = 7$) were sacrificed by cervical dislocation under anesthesia with inhalant isoflurane. Pancreata were collected and fixed in 10% buffered formalin for 3 days and treated with 70% ethanol for 1 day before paraffin embedding at the Molecular Pathology Core Facility, Robarts Research Institute, Western University. The paraffin-embedded blocks were longitudinally sectioned in 5 μm slices and fixed onto glass microscope slides. The samples were de-paraffinized by graded washes using xylene, ethanol and PBS. Background Sniper (Cat# BS966H, Biocare Medical) was used to reduce non-specific background staining. Samples were incubated with primary antibodies against glucagon (1:500), Stmn2 (1:250), insulin (Cat# ab7842, Abcam; 1:250) and TGN46 (Cat# ab16059, Abcam; 1:200) and followed by secondary antibodies of goat anti-mouse IgG Alexa Fluor 488 (1:500), donkey anti-goat IgG Alexa Fluor 555 (1:500), and goat anti-guinea pig IgG Alexa Fluor 647 (Cat# A21450, Invitrogen; 1:500). Nuclei were stained with DAPI (1:1000), and tissues were mounted in Prolong

Antifade mountant (Cat# P36982, Thermo Fisher Scientific). As a background control for Stmn2, islet staining for Stmn2 was done using only the secondary antibody.

Image Acquisition

High-resolution images were acquired through a Nikon A1R Confocal microscope with a ×60 NA plan-Apochromat oil differential interference contrast objective and NIS-Elements software (Nikon, Mississauga, Canada) using a pinhole of 1 Airy unit. Images were sampled according to Nyquist criteria, and images of the Nyquist-cropped areas were captured at 1,024 × 1,024 pixel resolution, and deconvoluted by the 2D- deconvolution algorithm of the NIS-Elements software, thereby optimizing images for accurate co-localization of fluorescent signals.

Image Analysis

For cell image analysis, we prepared three coverslips for each group. Image analysis was performed by NIS-Elements software (Nikon, Mississauga, Canada), using the co-localization option and Pearson's correlation coefficient (PCC). Regions of interest (ROI) were manually drawn around distinct single or multicellular bodies, and merged values of glucagon and Stmn2 were taken for analysis. Colocalization of the pixels from each pseudo-colored image was used to calculate Pearson's correlation coefficient, as we described previously (25, 31).

For mouse pancreatic islets, images were captured using four channels of green (glucagon), red (Stmn2), purple (insulin) and blue (nucleus; DAPI). To calculate the extent of co-localization between glucagon and stathmin-2 (glucagon$^+$, Stmn2$^+$), images of 15 islets per pancreas were captured and analyzed by Pearson's correlation coefficient (PCC). To this end, we manually drew ROIs around each islet and then defined PCC values for colocalization between Stmn2 and glucagon or insulin using the colocalization option of the NIS-Elements software. To predict expression levels of Stmn2 in α or β- cells of the pancreatic islets we have performed binary analysis using M-Thresholding algorithm of NIS-Elements software, followed by regression analysis of Stmn2 vs. glucagon or insulin using GraphPad Prism 7.

Immunoelectron Microscopy

Double immunogold transmission electron microscopy was done based on the protocol by Aida et al. (32) with some modifications. Briefly, pieces of mouse pancreata were cut and immediately placed into McDowell Trump's fixative (Cat# 18030-10; Electron Microscopy Sciences) for 1h. Then, after washing with PBS, samples were dehydrated in increasing concentrations of ethanol (10, 20, 30, 50, 70, 90, 100, and 100%) at 30 min per concentration. We followed the following protocol for LR White embedding and incubation: Incubation in ethanol-LR White mixture (3:1, v/v; 2 h), ethanol-LR White (1:1, v/v; 8 h), ethanol-LR White mixture (1:3, v/v; 12 h), pure LR White mixture (12 h), pure LR White (12 h) and pure LR White (12 h). The sample was then placed into a beem capsule, filled with pure LR White and incubated at 50°C for 24 h. Semi-thin sections (500 nm) were cut from the embedded sample for Toluidin blue staining (1% Toluidin blue for 2 min). By defining the position of the islets, ultra-thin sections (70 nm) were prepared using a diamond microtome. The sections were mounted on formvar-carbon coated nickel grid (300 meshes) (Cat# FCF300-NI, Electron Microscopy Sciences). Then, slices were washed with Tris-buffered saline (Tris 1M, NaCl 5M pH 8) containing 0.05% Tween 20 (TBS-T) and incubated in blocking buffer (2% BSA in PBS plus 0.05% Tween 20) for 30 min at room temperature. Slices were incubated with primary antibodies (1:10 in blocking buffer) against glucagon (Cat# ab92517; Abcam) and Stmn2 (Cat# ab115513; Abcam) at 4°C overnight. After washing with TBS-T, slices were incubated with gold conjugated secondary antibodies (1:50 in blocking buffer) of donkey anti-goat IgG (18 nm; cat# ab105270, Abcam) and goat anti-rabbit IgG (10 nm; Cat# ab27244; Abcam) for 2 h at room temperature. After washing with TBS-T and staining with Uranyless (Cat# 22409, Electron Microscopy Sciences), transmission electron microscopy was conducted at the Biotron Experimental Research Center, Western University, London, ON, Canada.

Primary Islet Culture

Islet preparation and culture was done according to the Li et al. (33) protocol with some modifications. Male C57BL/6 mice (n = 5–6) were euthanized by CO2. The abdominal cavity was opened and 3 mL of 1.87 mg/mL collagenase V (Cat# C9263, Sigma;) in Hanks' Balanced Salt Solution was injected into the common bile duct. The pancreas was then removed, placed into a Falcon tube containing 2 mL of the ice-cold collagenase V solution and incubated for 12 min at 37°C with occasional shaking. Digestion was stopped by adding 1mM $CaCl_2$ and the cell suspension was washed twice in the $CaCl_2$ solution. Islets were collected into a sterile petri dish using a 70 μm cell strainer with RPMI1640 containing 11 mM glucose plus 20 mM glutamine, 10% FBS and penicillin (110 U/mL) and streptomycin (100 μg/mL). 180 islets were handpicked into the medium under a stereomicroscope and incubated for 2 h in the cell culture incubator. The medium was then changed to RPMI1640 containing 11 mM glucose plus 10% FBS and penicillin (110 U/mL) and streptomycin (100 μg/mL) and cultured overnight at 37°C.

Islet Glucagon Secretion Experiments

Glucagon secretion from islets was measured based on the protocol by Suckow et al. (34). Briefly, islets were washed three times using Krebs-Ringer bicarbonate (KRB) buffer (135 mM NaCl, 3.6 mM KCl, 5 mM $NaHCO_3$, 0.5 mM NaH_2PO_4, 0.5 mM $MgCl_2$, 1.5 mM $CaCl_2$, 10 mM HEPES; pH 7.4) containing 11 mM glucose, and then pre-incubated in this buffer for 1 h. Glucagon secretion was tested by incubating islets in KRB containing 1 mM glucose in the presence or absence of arginine (25 mM) for 20 min. Media were collected into microcentrifuge tubes containing enzyme inhibitors (PMSF, 45 mM; Aprotinin, 5 μg/mL and sodium orthovanadate, 1 mM). Samples were centrifuged at 14,000 × g for 5 min at 4°C and the supernatant was collected and kept at −80°C until analysis.

Measurement of Glucagon and Stathmin-2

Glucagon levels in the media were determined by ELISA (Cat # EHGCG, Thermo Fisher Scientific) according to the

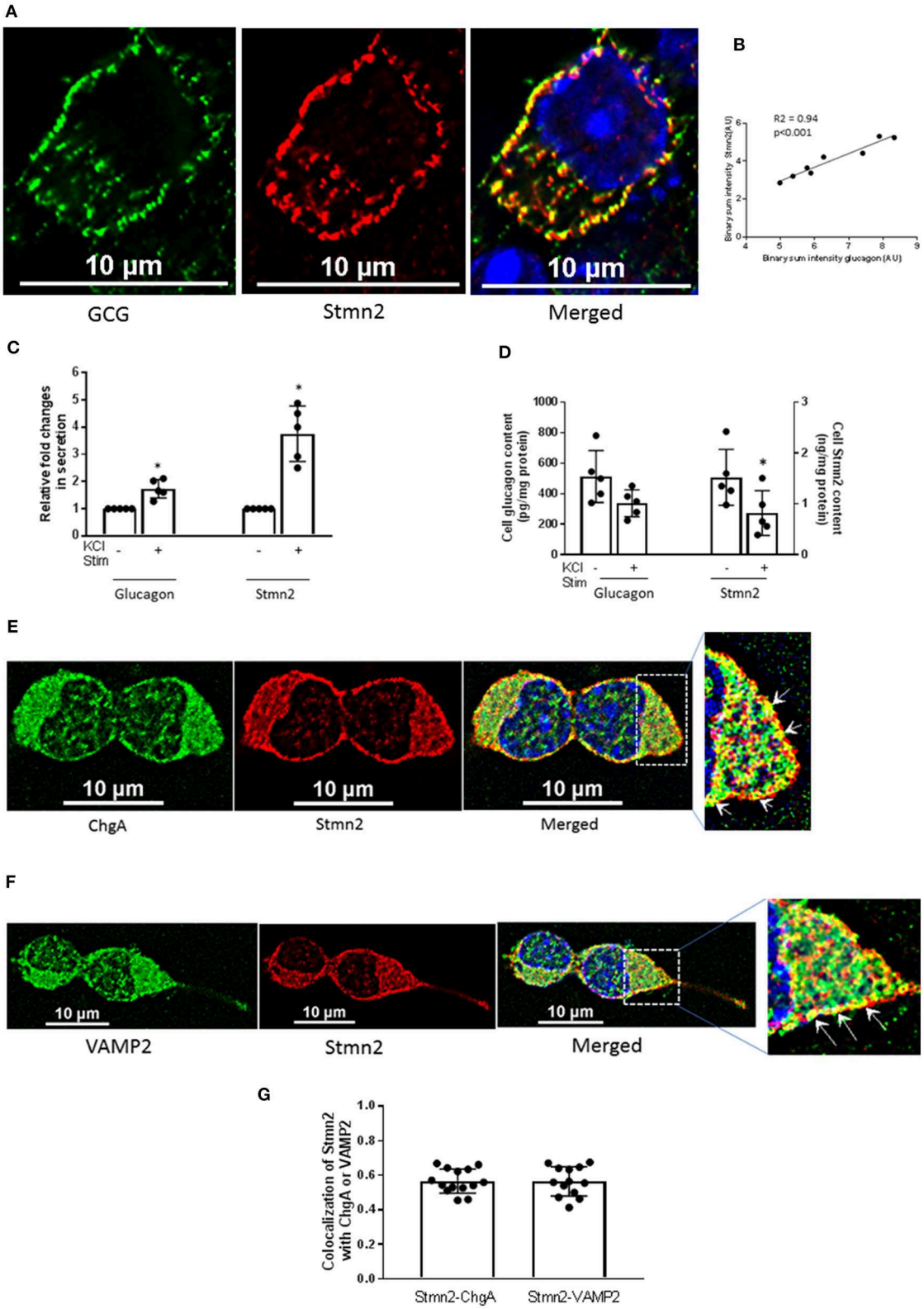

FIGURE 1 | Stathmin-2 localizes to secretory granules in αTC1-6 cells. αTC1-6 cells were immunostained using primary antibodies against glucagon (GCG, green) and stathmin-2 (Stmn2, red). DAPI (blue) indicates the nucleus in the merged image. Resolution of the images was extended by applying Nyquist XY scan and then

(Continued)

FIGURE 1 | 2D- Deconvolution in NIS Elements image analysis software. Images are representative of four biological replicates with 3 technical replicates each. **(A)** Areas of yellow in the merged image show colocalization of glucagon and Stmn2. **(B)** Linear regression analysis of binary intensities of glucagon and Stmn2 predicts a significant ($p < 0.001$) correlation. Each value represents mean intensities of 5-7 cells. The secretion of both glucagon and Stmn2 **(C)** was significantly increased after KCl stimulation (KCl Stim)for 15 min. **(D)** Cell Stmn2 and glucagon levels show reduction following KCl stimulation (KCl Stim). Values are expressed as mean ± SEM ($n = 5$). *$p < 0.05$. Stmn2 colocalizes with the secretory granule proteins ChgA **(E)** and VAMP2 **(F)**, as indicated by yellow punctate staining. **(G)** The extent of colocalization was analyzed by Pearson correlation coefficient for Stmn2 with ChgA or with VAMP2.

manufacturer's instructions. Stmn2 levels in the media were measured using mouse stathmin-2 ELISA kit (Cat# MBS7223765, MyBioSource) according to the manufacturer's instruction. For each measurement, the values were compared between groups by *t*-test and among groups by 1-Way ANOVA and Bonferroni *post-hoc* test ($\alpha = 0.05$). Cell protein levels were determined using BCA assay and used for normalization of the glucagon or Stmn2 levels.

Statistical Analysis

Values were compared among treatment groups by one-way ANOVA or between groups by unpaired *t*-test using Sigma Stat 3.5 software ($\alpha = 0.05$). For image analysis, co-localization of channels in the merged images was calculated by Pearson's correlation coefficient (PCC) using NIS-Elements software (Nikon, Canada).

RESULTS

Stmn2 Co-localizes With Glucagon and Secretory Granule Markers in αTC1-6 Cells

Immunostaining of glucagon and Stmn2 in αTC1-6 cells revealed significant co-localization, as shown in **Figure 1A** and by a positive Pearson's correlation coefficient (0.74 ± 0.05) between endogenously expressed glucagon and Stmn2. Linear regression of binary intensities showed a sensitive and significant relationship between colocalization of glucagon and Stmn2 (**Figure 1B**). The secretion of both glucagon and Stmn2 was significantly enhanced in response to 55 mM K^+ (**Figure 1C**), with corresponding decreases in cell contents (**Figure 1D**). To further confirm the presence of stathmin-2 in secretory granules, αTC1-6 cells were immunostained for stathmin-2 and the secretory granule markers chromogranin A (**Figure 1E**) and VAMP2 (**Figure 1F**). There was moderate colocalization (35) between Stmn2 and chromogranin A (PCC 0.58 ± 0.07) or VAMP2 (PCC 0.56 ± 0.09) (**Figure 1G**), indicating that Stmn2 is partially localized to the secretory granule compartment in αTC1-6 cells.

Stathmin-2 Localizes to the α Cell Secretory Pathway in Mouse Pancreatic Islets

Immunostaining of mouse pancreatic islets showed a pattern of Stmn2 immunofluorescence similar to that of glucagon, and not insulin (**Figure 2A**). Analysis by Pearson correlation showed a strong colocalization between glucagon and Stmn2 in the islets (PCC = 0.77 ± 0.02), but not between insulin and Stmn2 (**Figure 2B**). Linear regression analysis of the binary intensities revealed a very strong and significant relationship between Stmn2 and glucagon immunofluorescence (**Figure 2C**), while there was no significant relationship between Stmn2 and insulin (**Figure 2D**). There was also a strong relationship between Stmn2 and the *trans* Golgi marker, TGN46 (PCC = 0.72 ± 0.09) in both islet clusters (**Figure 2E**) and mature islets (**Figure 2F**). In addition, double immunogold-labeling TEM revealed the presence of both glucagon and Stmn2 within secretory granules of pancreatic α-cells. The co-localization of glucagon (10 nm particles; white arrows) and Stmn2 (18 nm particles; black arrows) was mostly within the core area of the secretory granules (**Figure 3A**). Finally, 25 mM Arg significantly enhanced the secretion of both glucagon and Stmn2 from isolated islets (**Figure 3B**). These results indicate that Stmn2 is localized to the secretory pathway of α cells in mouse pancreatic islets.

Effects of Depletion and Overexpression of Stmn2 on Glucagon Secretion

In order to determine if Stmn2 had any functional effects in α-cells, we manipulated levels of Stmn2 and measured K^+-stimulated glucagon secretion. Following siRNA-mediated knockdown of Stmn2 in αTC1-6 cells, basal secretion of glucagon was increased ∼4.5-fold, and was not significantly different from K^+-stimulated secretion (**Figure 4A**), indicating increased constitutive secretion. Efficacy of siRNA-mediated depletion of Stmn2 was shown by a significant reduction ($p < 0.01$) in Stmn2 mRNA levels (**Figure 4B**) and the Stmn2 immunoreactive band by western blot (**Figure 4C**). As well, silencing of Stmn2 did not affect proglucagon gene expression levels (**Figure 4D**), indicating that the effects of Stmn2 depletion were on glucagon secretion alone. Conversely, overexpression of Stmn2 dramatically reduced both basal and stimulated glucagon secretion compared to the corresponding control groups (**Figure 4E**; $p < 0.001$). These findings suggest that Stmn2 levels may control the regulated secretion of glucagon from αTC1-6 cells.

Stmn2 Directs Glucagon Into Early Endosomes

In wild type αTC1-6 cells, there was weak co-localization between glucagon and the early endosome marker EEA1 (**Figure 5A**) (PCC = 0.15 ± 0.02). When Stmn2 was overexpressed (**Figure 5B**), the extent of colocalization between glucagon and EEA1 increased markedly (PCC = 0.53±0.08). Depletion of Stmn2 (**Figure 5C**) drastically reduced the extent of colocalization (PCC = 0.05) between glucagon and EEA1. Pearson's correlation coefficient of co-localization between glucagon and Stmn2 showed a significant increase when Stmn2 was overexpressed ($p < 0.001$) and a significant reduction when Stmn2 was knocked down ($p < 0.05$) compared to the control (**Figure 5D**). These findings suggest that Stmn2 plays a role in directing glucagon toward early endosomes.

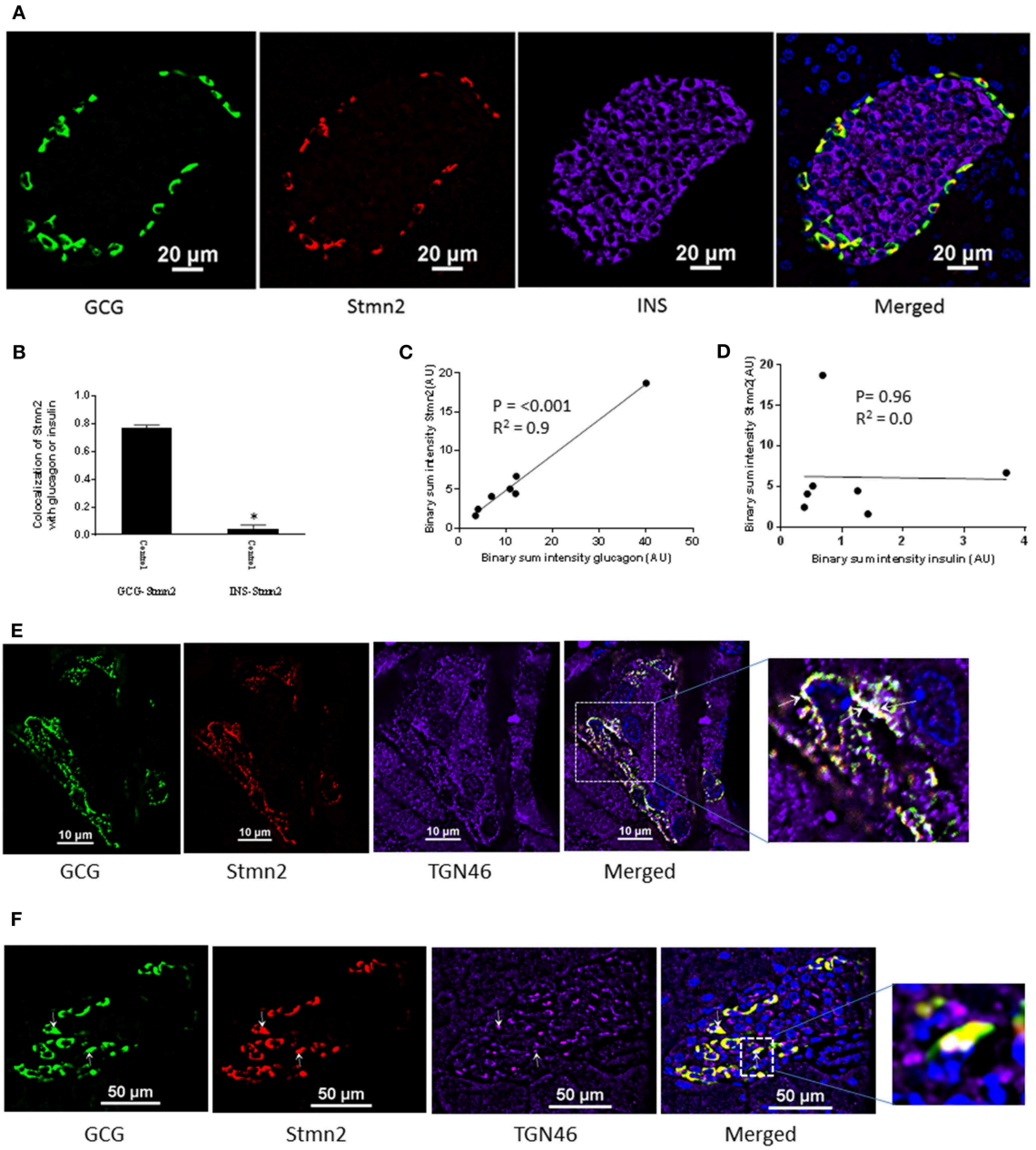

FIGURE 2 | Stathmin-2 is present in α-cells, but not β cells, in murine pancreatic islets. Pancreata of C57BL/6 mice ($n = 7$; 5 µm sections) were immunostained for glucagon (GCG), stathmin-2 (Stmn2) and insulin (INS). Images were acquired and analyzed for co-localization as described in **Figure 1**. **(A)** Both glucagon and Stmn2 localize to the mantle of the islets, and areas of yellow in the merged image demonstrate dual positive alpha cells (glucagon$^+$ and Stmn2$^+$). **(B)** Pearson's correlation coefficient for colocalization of Stmn2 and glucagon or insulin. **(C)** Linear regression analysis predicts a strong positive correlation between the binary intensities of glucagon and Stmn2 ($p < 0.001$). **(D)** There is no correlation between the binary intensities of insulin and Stmn2. **(E,F)** Colocalization of Stmn2 and the trans-Golgi marker TGN46 in murine pancreatic islets. Areas of white (arrows in the magnified panel) indicate co-localization of glucagon, Stmn2 and TGN46 in islet clusters **(E)** and a single islet **(F)**.

Stmn2 Overexpression Increases Glucagon Presence in the Late Endosome/Lysosome Compartment

Similar to our findings in early endosomes, there was a weak correlation between glucagon and the late endosome-lysosome marker, Lamp2A (PCC = 0.2 ± 0.02) in wild type αTC1-6 cells (**Figures 6A,D**). Following overexpression of Stmn2, the levels of colocalization between glucagon and Lamp2A were significantly increased (PCC = 0.89 ± 0.05, $p < 0.001$) (**Figures 6B,D**). Depletion of Stmn2 significantly reduced the extent of colocalization between glucagon and Lamp2A compared to wild type cells (PCC = 0.001, $p < 0.01$)

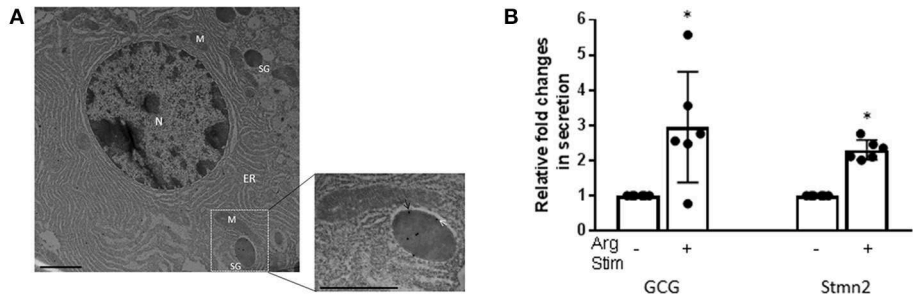

FIGURE 3 | Glucagon and Stmn2 are present within secretory granules of pancreatic α-cells. **(A)** Immunogold labels for both glucagon (10 nm; white arrows) and Stmn2 (18 nm; black arrows) are localized within secretory granules. The low magnification image (25,000×, scale bar = 1 μm) shows the ultrastructure of one alpha cell. N (nucleus); M (mitochondria); ER (endoplasmic reticulum); SG (secretory granule). The magnified image (41,000×, scale bar = 0.6 μm) highlights the presence of immunogold labels within a single secretory granule. **(B)** Isolated mouse islets were incubated in the presence or absence of 25 mM Arg for 20 min. Both glucagon and Stmn2 secretion from murine islets is stimulated by arginine. Values were normalized to the non-stimulated condition and expressed as mean ± SEM ($n = 5$–6). *$p < 0.01$.

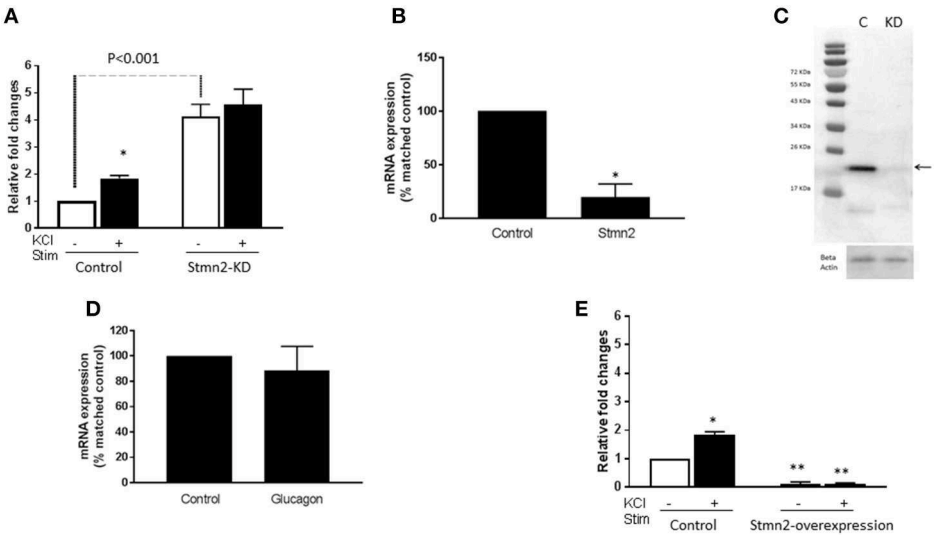

FIGURE 4 | Silencing Stathmin-2 increased glucagon secretion and overexpression of stathmin-2 suppressed glucagon secretion in αTC1-6 cells. Wild type (wt; control) and stathmin-2 depleted (Stmn2-KD) aTC1-6 cells were pre-incubated 2 h in serum-free medium and then incubated with or without KCl (55 mM) for 15 min. **(A)** Glucagon secretion is significantly stimulated by KCL in wt cells, while in Stmn-KD cells, basal glucagon secretion is increased and does not respond to KCl. *$p < 0.01$ compared to basal secretion in wt cells. **(B)** Stmn2 mRNA levels are decreased by about 70% after siRNA-mediated depletion in αTC1-6 cells. Values are means ± SEM ($n = 5$), *$p < 0.01$. **(C)** Stathmin-2 protein levels are depleted after siRNA-mediated silencing of Stmn2. C (control); KD (gene silenced). Beta-actin was used as a loading control. **(D)** Proglucagon mRNA levels are not affected by siRNA-mediated depletion of stathmin-2. **(E)** Glucagon secretion is inhibited by overexpression of Stmn2. αTC1-6 cells were transfected with pcDNA3.1 (+) MAr-stmn2 or empty vector (negative control). Both basal and K^+-stimulated glucagon secretion were inhibited by overexpression of Stmn2. Values are means ± SEM ($n = 4$). *$p < 0.05$; **$p < 0.001$ compared to unstimulated control.

(**Figures 6C,D**). Interestingly, the signal intensity of the endo-lysosomal marker, Lamp2A, was significantly increased ($p < 0.01$) upon overexpression of Stmn2, but did not change upon depletion of Stmn2 (**Figure 6E**).

DISCUSSION

Glucagon secretion is governed by systemic, paracrine and intrinsic factors. Our work has focused on the regulation of glucagon secretion by proteins that associate with glucagon within alpha cell secretory granules. To this end, we have shown that a neuronal protein, Stmn2, which we have previously identified as part of the glucagon interactome (25), can be localized to the secretory granules of αTC1-6 cells. We validated this association in mouse pancreatic islets, and through silencing and overexpression experiments, we showed that Stmn2 can play a role in glucagon secretion by trafficking through the endosomal-lysosomal pathway.

We have previously identified Stmn2 as part of a network of proteins that associate with glucagon within the secretory granules of αTC1-6 cells (25). Data in the current study show that Stmn2 is localized to the secretory granule and Golgi

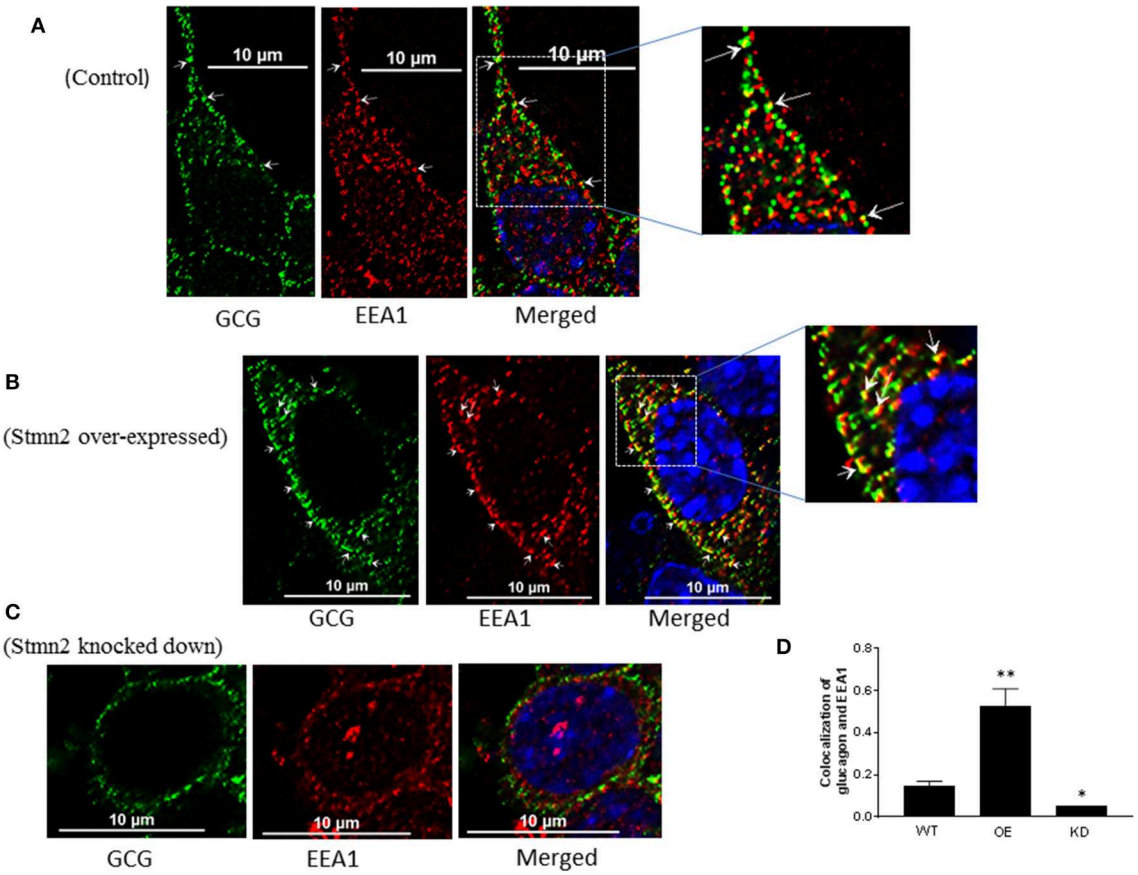

FIGURE 5 | Stathmin-2 modulates glucagon trafficking through early endosomes. After transfection with either empty vector **(A)**, vector encoding Stmn2 **(B)** or siRNAs against Stmn2 **(C)**, αTC1-6 cells were immunostained using primary antibodies against glucagon and the early endosome marker EEA1. Images were acquired and analyzed for co-localization as described in **Figure 1**. Colocalization of glucagon and EEA1 (yellow puncta) are indicated by arrows in wt cells **(A)** or arrowheads in cells overexpressing Stmn2 **(B)**. **(D)** Level of colocalization between glucagon and EEA1 was determined by Pearson's correlation coefficient in wt cells, cells in which Stmn2 was overexpressed (OE) and in which Stmn2 was knocked down by siRNA (KD). Values were expressed as mean ± SEM ($n = 5$) and compared by 1-Way ANOVA. *$p < 0.05$; ** < 0.001 compared to wt.

compartments in αTC1-6 cells and mouse pancreatic alpha cells, respectively. Stathmin 2 is part of a family of neuronal phosphoproteins that associates with intracellular membranes, notably the Golgi and vesicle transporters, in neurons (36). Although Stmn2 has been identified as a neuron-specific protein that functions in differentiation and development, its presence in pancreatic alpha cells is not surprising, as several types of neuronal proteins, such as SNARE proteins, neurotransmitters and granins, are also expressed in endocrine cells (37–39). The expression of neuronal proteins such as Stmn2 in alpha cells may be due to the absence of the transcriptional repressor RE-1 silencing transcription factor (REST) in mature endocrine cells (40, 41). The absence of Stmn2 in mouse pancreatic beta cells suggests that transcriptional silencing programs may operate in a cell-specific manner.

Our results indicate that Stmn2 is localized largely to punctate structures within αTC1-6 cells, notably at the plasma membrane. Its colocalization with glucagon, ChGA and VAMP2 at the plasma membrane suggests that it is efficiently sorted from the Golgi to plasma membrane-associated secretory granules. Double immunogold labeling TEM confirmed the presence of glucagon and Stmn2 within secretory granules of α-cells in mouse pancreatic islets. The presence of Stmn2 within the dense core of the granule suggests that it is part of the soluble granule cargo along with glucagon. These results are consistent with our secretory granule proteomics, which predicted the presence of both glucagon and Stmn2 in secretory granules of αTC1-6 cells (25). Our model also predicted that the complement of proteins within alpha cell secretory granules differs in response to microenvironmental inputs, so it possible that Stmn2 is present only in a subpopulation of secretory granules. The trafficking of Stmn2 to secretory granules in αTC1-6 cells may occur through specific molecular domains within its sequence. The subcellular trafficking pattern of Stmn2 in neurons and neuroendocrine cells is determined by its N-terminal extension, which contains a Golgi localization domain and a membrane anchoring domain that contains two conserved Cys residues as sites for palmitoylation (36). This lipid modification occurs in the Golgi (42) and is

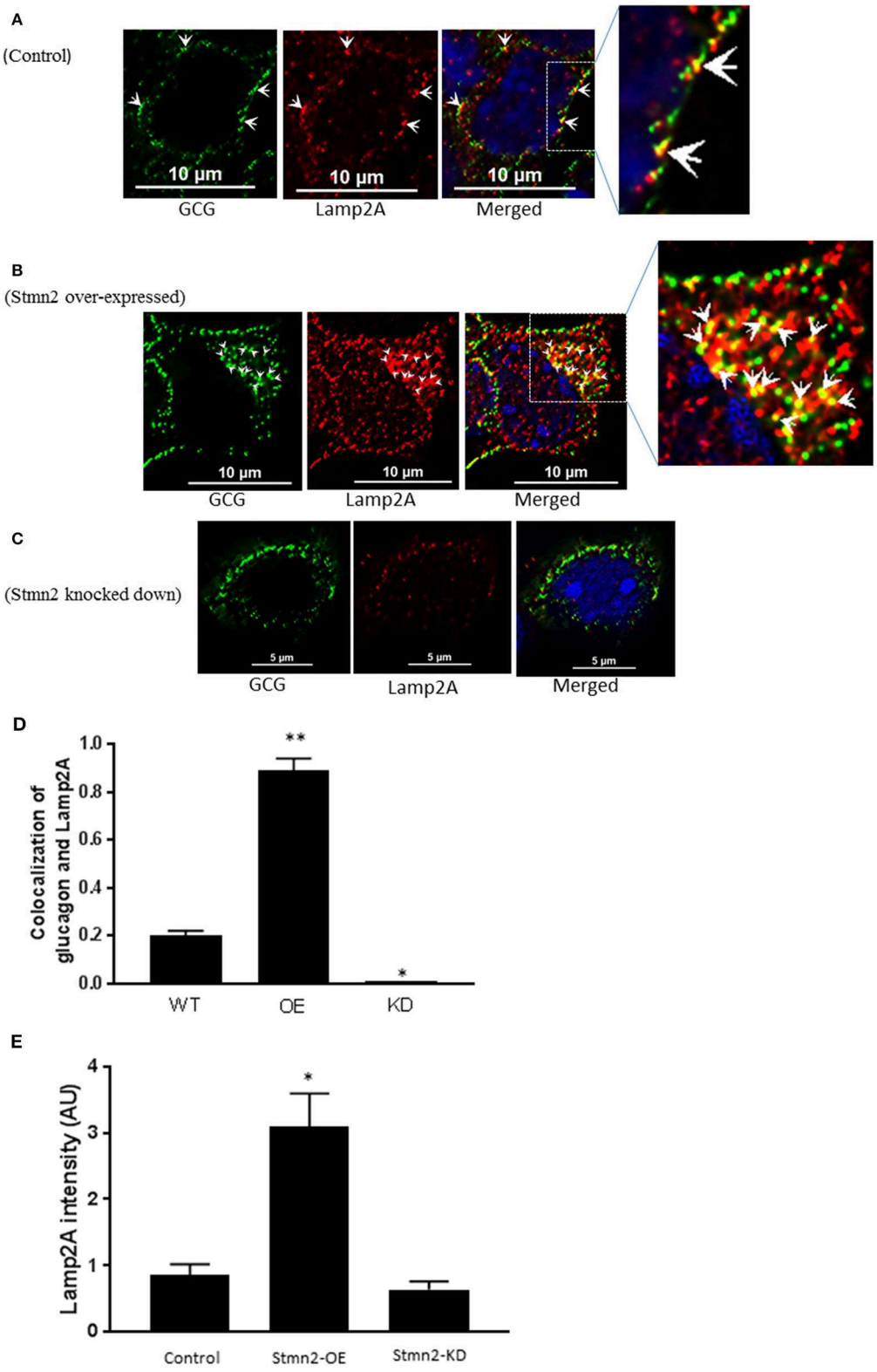

FIGURE 6 | Overexpression of Stathmin-2 increases the presence of glucagon in late endosomes/lysosomes. After transfection with either empty vector **(A)**, vector encoding Stmn2 **(B)** or siRNAs against Stmn2 **(C)**, αTC1-6 cells were immunostained using primary antibodies against glucagon and the late endosome-lysosome *(Continued)*

FIGURE 6 | marker LAMP2A. Images were acquired and analyzed for co-localization as described in **Figure 1**. **(A)** In wt cells, glucagon and LAMP2 show some co-localization at the plasma membrane (arrowheads). **(B)** In cells overexpressing Stmn2, there is colocalization of glucagon and LAMP2A in the cell body (arrowheads) and at the plasma membrane (arrows). **(C)** In cells in which Stmn2 levels are depleted, there is almost no detectable co-localization of glucagon and LAMP2A. **(D)** Level of colocalization between glucagon and LAMP2A was determined by Pearson's correlation coefficient in wt cells, cells in which Stmn2 was overexpressed (OE) and in which Stmn2 was knocked down by siRNA (KD). **(E)** Fluorescence intensity of Lamp2A in wt cells, and following overexpression (Stmn2-OE) or knockdown (Stmn2-KD) of Stmn2. Values are expressed as mean ± SD and compared by 1-Way ANOVA. $^{*}p < 0.01$; $^{**} < 0.001$ compared to wt.

sufficient and necessary for the association of Stmn2 with Golgi membranes, and its sorting to post-Golgi vesicles (42, 43). While we have not directly shown that palmitoylation of these Cys residues is required for localization in secretory granules in αTC1-6 cells, it is likely that this is a conserved sorting mechanism in neuroendocrine cells.

Consistent with its localization within secretory granules, the secretion of both glucagon and Stmn2 was significantly enhanced in response to 55 mM K^+. Although there was a statistically significant response to KCl, αTC1-6 cells as a rule do not show robust secretory responses to KCl, glucose or other secretagogues. In general, αTC1-6 cells differ in their complement of transcriptional and epigenetic factors from mouse primary alpha cells, which may explain the relatively blunted secretory response seen in this cell line (44). The reduced response to glucose in particular could be due to a low efficiency in coupling between the glycolytic and TCA pathways, as has been shown in pancreatic islets (45). Nonetheless, we were able to show similar secretory behavior of glucagon and Stmn2 in isolated mouse islets, thus confirming their localization within the releasable pool of secretory granules in pancreatic α-cells. While Stmn2 is a membrane–bound protein, it is also present in normal human blood as determined by serum ELISA (46) and plasma proteomics (47) and therefore can be also secreted. There is some evidence of a lower molecular weight form of Stmn2 that may correspond to a cleaved, soluble form (43, 48). In our model, it may be that a portion of Stmn2 becomes cleaved within the secretory granule, thus becoming part of the soluble cargo that is released.

By manipulating the expression of Stmn2, we were able to demonstrate a role in the control of glucagon secretion. There is precedence for a role for Stmn2 in the regulation of neuroendocrine secretion that has some interesting parallels with our results. While we showed that silencing of Stmn2 increased the constitutive secretion of glucagon, one study showed that silencing Stmn2 in PC12 cells decreased both basal and stimulated secretion of chromogranin A (27). In that study, it was shown that Stmn2 interacted directly with ChgA and its depletion reduced the buoyant density of chromaffin granules, suggesting that Stmn2 may participate in secretory granule formation, perhaps in partnership with ChgA (42) and thus promote regulated secretion. Although we could not demonstrate a direct interaction between Stmn2 and glucagon (data not shown), our results align with the idea that Stmn2 may be a sorting partner for glucagon, perhaps by interacting with other granule proteins such as ChgA or carboxypeptidase E (31), in the regulated secretory pathway of alpha cells.

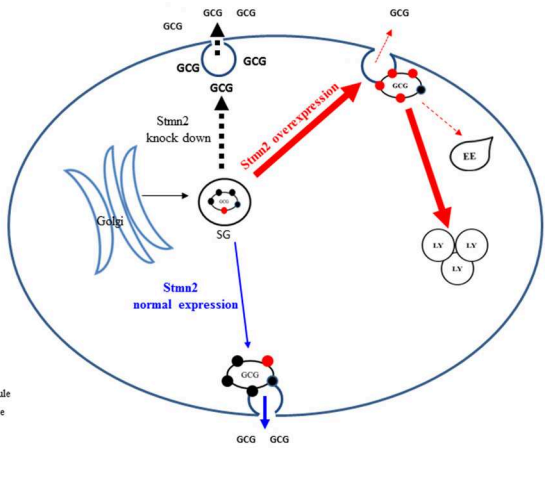

FIGURE 7 | Proposed pathways by which stathmin-2 modulates glucagon secretion from αTC1-6 cells. The model denotes status of glucagon secretion from αTC1-6 cells in normal physiology or in the event of Stmn2- depletion or overexpression. Blue arrows indicate the normal trafficking of glucagon, together with Stmn2, to secretory granules, where they are stored until their release is triggered by a stimulus. Stmn2 overexpression (red arrows) reduces the amount of glucagon available for secretion by diverting secretory granules to lysosomes. Stmn2 depletion (black arrows) reduces the trafficking of glucagon into secretory granules and promotes the constitutive release of glucagon.

Overexpression of Stmn2 resulted in an almost complete shutdown of glucagon secretion and an increase in the localization of glucagon in early endosomes and lysosomes. These results may suggest induction of ER stress. However, overexpression of Stmn2 in Neuro2A cells, another cell line commonly used to examine regulated secretion, had the opposite effect and enhanced trafficking of post-Golgi carriers to the plasma membrane (49). There are only a few reports on how ER stress in alpha cells is manifest; in one report, palmitate-induced ER stress in isolated rat alpha cells resulted in an increase in glucagon secretion, not inhibition, even though the traditional markers of ER stress [Ddit3 (Chop), Xbp1s, Hsp5a (BiP)] were elevated (50). Another study showed that *in vivo* depletion of Xbp1, which plays a crucial role in the unfolded protein response, induced dysfunctional glucagon secretion that was not fully suppressed by insulin (51). Therefore, the suppression of glucagon secretion by Stmn2 overexpression is not consistent with the phenotype of ER stress in the alpha cell. Instead, these results, together with the increased the presence of glucagon in the lysosomal compartment, suggest that

Stmn2 overexpression causes alterations in glucagon trafficking independent of ER stress.

We believe that the overexpression experiments suggest a mechanism whereby an increase in Stmn2 in the alpha cell inhibits glucagon secretion by targeting glucagon secretory granules for degradation in the endosome-lysosome pathway, perhaps in a manner similar to that of insulin secretory granules in Type 2 diabetes (52). Very recently, it has been shown that insulin secretion can be inhibited by the targeting of proinsulin for lysosomal degradation by Rab7-interacting lysosomal protein (RILP) (53). The proposed mechanism of action was through interactions between RILP and an insulin secretory granule membrane protein, Rab26. It is tempting to speculate that Stmn2 could have a similar mechanism of action in alpha cells. The increase in LAMP2 fluorescence intensity upon Stmn2 overexpression further suggests a role for Stmn2 in modulating glucagon secretion through increased lysosome function or biogenesis. We are currently investigating this mechanism of control of glucagon secretion in mouse islets.

In conclusion, we propose that Stmn2, a protein that is associated with glucagon in secretory granules, modulates glucagon secretion in alpha cells by playing a role in its intracellular trafficking. Under conditions that decrease Stmn2 levels, constitutive secretion of glucagon is increased; and under conditions that increase levels of Stmn2, glucagon is targeted to the endolysosomal system, presumably for degradation (**Figure 7**). Our findings, which are mainly based on the clonal α-cell line αTC1-6, represent a potentially novel intracellular pathway for the control of glucagon secretion, and may lead to new mechanistic insights in the dysregulation of glucagon secretion in diabetes.

DATA AVAILABILITY STATEMENT

All datasets generated for this study are included in the article/supplementary material.

ETHICS STATEMENT

The animal study was reviewed and approved by Animal Use Subcommittee of the Canadian Council on Animal Care at Western University, Animal Use Protocol AUP 2012-020.

AUTHOR CONTRIBUTIONS

Designing the experiments, writing the manuscript, preparing the figures and reviewing the manuscript prior to submission were done by FA and SD.

FUNDING

This work has been financially supported by a Discovery Grant from the Natural Sciences and Engineering Research Council of Canada to SD, and by a Dean's Award Scholarship to FA.

ACKNOWLEDGMENTS

We would like to sincerely thank Dr. Jens Juul Holst (Department of Biomedical Sciences, University of Copenhagen, Denmark) for reviewing the manuscript and providing constructive suggestions; Ms. Karen Nygard and Mr. Reza Khazaee for assistance with electron microscopy; and Ms. Caroline O'Neil for tissue sample sectioning.

REFERENCES

1. Ceriello A, Kilpatrick ES. Glycemic variability: both sides of the story. *Diabetes Care*. (2013) 36:S272–5. doi: 10.2337/dcS13-2030
2. Demant M, Bagger J, Suppli M, Lund A, Gyldenløve M, Hansen K et al. Determinants of fasting hyperglucagonemia in patients with type 2 diabetes and nondiabetic control subjects. *Metab Syndr Relat Disord*. (2018) 16:530–536. doi: 10.1089/met.2018.0066
3. Salehi A, Vieira E, Gylfe E. Paradoxical stimulation of glucagon secretion by high glucose concentrations. *Diabetes*. (2006) 55:2318–2323. doi: 10.2337/db06-0080
4. Vieira E, Salehi A, Gylfe E. Glucose inhibits glucagon secretion by a direct effect on mouse pancreatic alpha cells. *Diabetologia*. (2007) 50:370–379. doi: 10.1007/s00125-006-0511-1
5. Gylfe E, Gilon P. Glucose regulation of glucagon secretion. *Diabetes Res Clin Pract*. (2014) 103:1–10. doi: 10.1016/j.diabres.2013.11.019
6. Gylfe E. Glucose control of glucagon secretion—'There's a brand-new gimmick every year.' *Ups J Med Sci*. (2016) 9734:1–13. doi: 10.3109/03009734.2016.1154905
7. Brand C, Rolin B, JØrgensen P, Svendsen I, Kristensen JS, Holst JJ. Immunoneutralization of endogenous glucagon with monoclonal glucagon antibody normalizes hyperglycaemia in moderately streptozotocin-diabetic rats. *Diabetologia*. (1994) 37:985–93. doi: 10.1007/BF00400461
8. Gelling RW, Du XQ, Dichmann DS, Romer J, Huang H, Cui L, et al. Lower blood glucose, hyperglucagonemia, and pancreatic alpha cell hyperplasia in glucagon receptor knockout mice. *Proc Natl Acad Sci USA*. (2003) 100:1438–43. doi: 10.1073/pnas.0237106100
9. Holst JJ, Albrechtsen NJW, Pedersen J, Knop FKG. Glucagon and amino acids are linked in a mutual feedback cycle: the liver-α-cell axis. *Diabetes*. (2017) 66:235–40. doi: 10.2337/db16-0994
10. Longuet C, Sinclair EM, Maida A, Baggio LL, Charron MJ, Drucker DJ. The glucagon receptor is required for the adaptive metabolic response to fasting. *Cell Metab*. (2009) 8:359–71. doi: 10.1016/j.cmet.2008.09.008
11. Unger RH, Cherrington AD. Glucagonocentric restructuring of diabetes: a pathophysiologic and therapeutic makeover. *J Clin Invest*. (2012) 122:4–12. doi: 10.1172/JCI60016
12. Gromada J, Chabosseau P, Rutter GA. The α-cell in diabetes mellitus. *Nat Rev Endocrinol*. (2018) 14:694–704. doi: 10.1038/s41574-018-0097-y
13. Ramracheya R, Chapman C, Chibalina M, Dou H, Miranda C, González A, et al. GLP-1 suppresses glucagon secretion in human pancreatic alpha-cells by inhibition of P/Q-type Ca2+ channels. *Physiol Rep*. (2018) 6:1–17. doi: 10.14814/phy2.13852
14. Tornehave D, Kristensen P, Rømer J, Knudsen LB, Heller RS. Expression of the GLP-1 receptor in mouse, rat, and human pancreas. *J Histochem Cytochem*. (2008) 56:841–51. doi: 10.1369/jhc.2008.951319
15. Benner C, van der Meulen T, Cace'res E, Tigyi K, Donaldson CJ, Huising MO. The transcriptional landscape of mouse beta cells compared to human beta cells reveals notable species differences in long non-coding RNA and protein-coding gene expression. *BMC Genomics*. (2014) 15:620. doi: 10.1186/1471-2164-15-620
16. Ørgaard A, Holst JJ. The role of somatostatin in GLP-1-induced inhibition of glucagon secretion in mice. *Diabetologia*. (2017) 60:1731–9. doi: 10.1007/s00125-017-4315-2
17. Kawamori D, Kulkarni RN. Insulin modulation of glucagon secretion: the role of insulin and other factors in the regulation of glucagon secretion. *Islets*. (2009) 1:276–9. doi: 10.4161/isl.1.3.9967

18. Rorsman P, Berggren P, Bokvist K, Ericson H, Möhler H, Ostenson C, et al. Glucose-inhibition of glucagon secretion involves activation of GABAA-receptor chloride channels. *Nature*. (1989) 341:233–6. doi: 10.1038/341233a0
19. Basco D, Zhang Q, Salehi A, Tarasov A, Dolci W, Herrera P, et al. α-cell glucokinase suppresses glucose-regulated glucagon secretion. *Nat Commun*. (2018) 9:546. doi: 10.1038/s41467-018-03034-0
20. Knudsen J, Hamilton A, Ramracheya R, Tarasov A, Brereton M, Haythorne E, et al. Dysregulation of glucagon secretion by hyperglycemia-induced sodium-dependent reduction of ATP production. *Cell Metab*. (2019) 29:430–442. doi: 10.1016/j.cmet.2018.10.003
21. González-Vélez V, Dupont G, Gil A, González A, Quesada I. Model for glucagon secretion by pancreatic α-cells. *PLoS ONE*. (2012) 7:e32282. doi: 10.1371/journal.pone.0032282
22. Wendt A, Birnir B, Buschard K, Gromada J, Salehi A, Sewing S, et al. Glucose inhibition of glucagon secretion from rat α-cells is mediated by GABA released from neighboring β-cells. *Diabetes*. (2004) 53:1038–45. doi: 10.2337/diabetes.53.4.1038
23. Rorsman P, Ashcroft FM. Pancreatic β-Cell electrical activity and insulin secretion: of mice and men. *Physiol Rev*. (2018) 98:117–214. doi: 10.1152/physrev.00008.2017
24. Le Marchand SJ, Piston DW. Glucose suppression of glucagon secretion: metabolic and calcium responses from α-cells in intact mouse pancreatic islets. *J Biol Chem*. (2010) 285:14389–98. doi: 10.1074/jbc.M109.069195
25. Asadi F, Dhanvantari S. Plasticity in the glucagon interactome reveals proteins that regulate glucagon secretion in alpha TC1-6 cells. *Front Endocrinol*. (2019) 9:792. doi: 10.3389/fendo.2018.00792
26. Charbaut E, Chauvin S, Enslen H, Zamaroczy S, Sobel A. Two separate motifs cooperate to target stathmin-related proteins to the Golgi complex. *J Cell Sci*. (2005) 118:2313–23. doi: 10.1242/jcs.02349
27. Mahapatra NR, Taupenot L, Courel M, Mahata SK, O'Connor DT. The trans-golgi proteins SCLIP and SCG10 interact with chromogranin A to regulate neuroendocrine secretion. *Biochemistry*. (2008) 47:7167–78. doi: 10.1021/bi7019996
28. Bramswig N, Everett L, Schug J, Dorrell C, Liu C, Luo Y, et al. Epigenomic plasticity enables human pancreatic alpha to beta cell reprogramming. *J Clin Invest*. (2013) 123:1275–84. doi: 10.1172/JCI66514
29. Lawlor N, George J, Bolisetty M, Kursawe R, Sun L, Sivakamasundari V, et al. Single-cell transcriptomes identify human islet cell signatures and reveal cell-type – specific expression changes in type 2 diabetes. *Genome Res*. (2017) 27:208–22. doi: 10.1101/gr.212720.116
30. Mossé Y, Laudenslager M, Longo L, Cole K, Wood A, Attiyeh E, et al. Identification of ALK as the major familial neuroblastoma predisposition gene. *Nature*. (2009) 455:930–5. doi: 10.1038/nature07261
31. Guizzetti L, McGirr R, Dhanvantari S. Two dipolar alpha-helices within hormone-encoding regions of proglucagon are sorting signals to the regulated secretory pathway. *J Biol Chem*. (2014) 289:14968–80. doi: 10.1074/jbc.M114.563684
32. Aida K, Saitoh S, Nishida Y, Yokota S, Ohno S, Mao X, et al. Distinct cell clusters touching islet cells induce islet cell replication in association with over-expression of Regenerating Gene (REG) protein in fulminant type 1 diabetes. *PLoS ONE*. (2014) 9:e105449. doi: 10.1371/journal.pone.0095110
33. Li DS, Yuan YH, Tu HJ, Liang Q Le, Dail LJ. A protocol for islet isolation from mouse pancreas. *Nat Protoc*. (2009) 4:1649–52. doi: 10.1038/nprot.2009.150
34. Suckow AT, Polidori D, Yan W, Chon S, Ma JY, Leonard J, et al. Alteration of the glucagon axis in GPR120 (FFAR4) knockout mice: a role for gpr120 in glucagon secretion. *J Biol Chem*. (2014) 289:15751–63. doi: 10.1074/jbc.M114.568683
35. Zinchuk V, Wu Y, Grossenbacher-Zinchuk O. Bridging the gap between qualitative and quantitative colocalization results in fluorescence microscopy studies. *Sci Rep*. (2013) 3:1–5. doi: 10.1038/srep01365
36. Chauvin S, Sobel A. Neuronal stathmins: a family of phosphoproteins cooperating for neuronal development, plasticity and regeneration. *Prog Neurobiol*. (2015) 126:1–18. doi: 10.1016/j.pneurobio.2014.09.002
37. Franklin IK, Wollheim CB. GABA in the endocrine pancreas: its putative role as an islet cell paracrine-signalling molecule. *J Gen Physiol*. (2004) 123:185–90. doi: 10.1085/jgp.200409016
38. Daily NJ, Boswell KL, James DJ, Martin TFJ. Novel interactions of CAPS (Ca2+-dependent activator protein for secretion) with the three neuronal SNARE proteins required for vesicle fusion. *J Biol Chem*. (2010) 285:35320–9. doi: 10.1074/jbc.M110.145169
39. Schafer MKH, Mahata SK, Stroth N, Eiden LE, Weihe E. Cellular distribution of chromogranin A in excitatory, inhibitory, aminergic and peptidergic neurons of the rodent central nervous system. *Regul Pept*. (2010) 165:36–44. doi: 10.1016/j.regpep.2009.11.021
40. Atouf F, Czernichow P, Scharfmann R. Expression of neuronal traits in pancreatic beta cells. *J Biol Chem*. (1997) 272:1929–34. doi: 10.1074/jbc.272.3.1929
41. Martin D, Grapin-Botton A. The importance of REST for development and function of beta cells. *Front Cell Dev Biol*. (2017) 5:12. doi: 10.3389/fcell.2017.00012
42. Koshimizu H, Kim T, Cawley N, Loh Y. Chromogranin A: a new proposal for trafficking, processing and induction of granule biogenesis. *Regul Pept*. (2010) 165:95–101. doi: 10.1016/j.regpep.2010.09.006
43. Lutjens R, Igarashi M, Pellier V, Blasey H, Di Paolo G, Ruchti E, et al. Localization and targeting of SCG10 to the trans-Golgi apparatus and growth cone vesicles. *Eur J Neurosci*. (2000) 12:2224–34. doi: 10.1046/j.1460-9568.2000.00112.x
44. Lawlor N, Youn A, Kursawe R, Ucar D, Stitzel ML. Alpha TC1 and Beta-TC-6 genomic profiling uncovers both shared and distinct transcriptional regulatory features with their primary islet counterparts. *Sci Rep*. (2017) 7:1–14. doi: 10.1038/s41598-017-12335-1
45. Stamenkovic JA, Andersson LE, Adriaenssens AE, Bagge A, Sharoyko VV, Gribble F, et al. Inhibition of the malate–aspartate shuttle in mouse pancreatic islets abolishes glucagon secretion without affecting insulin secretion. *Biochem J*. (2015) 468:49–63. doi: 10.1042/BJ20140697
46. Kuttapitiya A, Assi L, Laing K, Hing C, Mitchell P, Whitley G, et al. Microarray analysis of bone marrow lesions in osteoarthritis demonstrates upregulation of genes implicated in osteochondral turnover, neurogenesis and inflammation. *Ann Rheum Dis*. (2017) 76:1764–73. doi: 10.1136/annrheumdis-2017-211396
47. Nanjappa V, Thomas J, Marimuthu A, Muthusamy B, Radhakrishnan A, Sharma R, et al. Plasma proteome database as a resource for proteomics research: 2014 update. *Nucleic Acids Res*. (2014) 42:959–65. doi: 10.1093/nar/gkt1251
48. Levy A, Devignot V, Fukata Y, Fukata M, Sobel A, Chauvin S. Subcellular Golgi localization of stathmin family proteins is promoted by a specific set of DHHC palmitoyl transferases. *Mol Biol Cell*. (2011) 22:1930–42. doi: 10.1091/mbc.e10-10-0824
49. Wang J, Shan C, Cao W, Zhang C, Teng J, Chen J. SCG10 promotes non-amyloidogenic processing of amyloid precursor protein by facilitating its trafficking to the cell surface. *Hum Mol Genet*. (2013) 22:4888–900. doi: 10.1093/hmg/ddt339
50. Marroqui L, Masini M, Merino B, Grieco FA, Millard I, Dubois C, et al. Pancreatic α cells are resistant to metabolic stress-induced apoptosis in type 2 diabetes. *EBioMedicine*. (2015) 2:378–85. doi: 10.1016/j.ebiom.2015.03.012
51. Akiyama M, Liew CW, Lu S, Hu J, Martinez R, Hambro B, et al. X-Box binding protein 1 is essential for insulin regulation of pancreatic α-cell function. *Diabetes*. (2013) 62:2439–49. doi: 10.2337/db12-1747
52. Pasquier A, Vivot K, Erbs E, Spiegelhalter C, Zhang Z, Aubert V, et al. Lysosomal degradation of newly formed insulin granules contributes to β cell failure in diabetes. *Nat Commun*. (2019) 10:1–14. doi: 10.1038/s41467-019-11170-4
53. Yuxia Z, Zhiyu L, Shengmei Z, Ruijuan Z, Huiying L, Xiaoqing L, et al. RILP restricts insulin secretion through mediating lysosomal degradation of proinsulin. *Diabetes*. (2020) 69:67–82. doi: 10.2337/db19-0086

Conflict of Interest: The authors declare that the research was conducted in the absence of any commercial or financial relationships that could be construed as a potential conflict of interest.